Hydrothermal Reactions of Formic Acid: Free-Energy Analysis of Equilibrium

Nobuyuki Matubayasi* and Masaru Nakahara

Institute for Chemical Research, Kyoto University, Uji, Kyoto 611-0011, Japan
*E-mail: nobuyuki@scl.kyoto-u.ac.jp

The chemical equilibria concerning formic acid are computationally investigated in water over a wide range of thermodynamic conditions. The solvation free energies for relevant C1 compounds are evaluated in the method of energy representation, and are used to assess the solvent effect on the formic acid reactions. In the two competitive decomposition processes of formic acid, the solvent strongly inhibits the decarboxylation ($HCOOH \longrightarrow CO_2 + H_2$), and its effect is relatively weak for the decarbonylation ($HCOOH \longrightarrow CO + H_2O$). The equilibrium weights for the two decomposition pathways of formic acid are determined by the equilibrium constant of the water-gas-shift reaction ($CO + H_2O \longrightarrow CO_2 + H_2$), which is an essential and useful process in fuel technology. The reaction control by the solvent is then examined for the water-gas-shift reaction. Through the comparison of the equilibrium constants in the absence and presence of solvent, even the favorable side of the reaction is shown to be tuned by the solvent density and temperature.

1. Introduction

Water is potentially a useful medium for organic chemical reactions. At ambient conditions, however, the utility of water as a reaction medium is restricted by the low solubility of organic compounds. Super- and subcritical water is a promising medium to overcome this restriction [1]. When the temperature is elevated and the density is not too high, water mixes well with organic compounds and often acts in a reaction both as an environment and as a reactant. A distinctive feature of super- and subcritical water is the availability of a wide range of density and temperature, and the role of water in an organic chemical reaction may be strongly dependent on the thermodynamic state. The reaction control in hydrothermal conditions is then possible only by clarifying the effect of the solvation at the molecular level [2]. Especially, the role of water in simplest organic reactions is the first subject to be investigated in detail toward a systematic construction of hydrothermal organic chemistry.

The simplest organic chemistry is the C1 chemistry, the chemistry of compounds with single carbon atom. Among the C1 compounds, formic acid is of particular interest for its rich reaction abilities. At high temperatures, formic acid decomposes through two competitive pathways expressed as

$$HCOOH \longrightarrow CO + H_2O \quad (1)$$

$$HCOOH \longrightarrow CO_2 + H_2 \quad (2)$$

Equations (1) and (2) generate carbon monoxide and carbon dioxide, respectively. In a recent series of papers, we showed that the competition between the decarbonylation (dehydration) and decarboxylation (dehydrogenation) of formic acid depends delicately on the condition of the system and that the decarbonylation is reversible in hydrothermal condition [3]. Formic acid is then a key intermediate of the water-gas-shift reaction [4] given by

$$CO + H_2O \longrightarrow CO_2 + H_2 \quad (3)$$

and its usage is suggested as a “chemical reservoir” for a clean fuel, H_2.

In the present work, we focus on the equilibrium constants of Eqs. (1)-(3) in water over a wide range of thermodynamic conditions. We evaluate the solvation free energies of the relevant species, and elucidate the effect of solvent density and temperature. We then construct the equilibrium constant in solution by combining the solvation free energies of the reactive species with their standard free energies of formation in the absence of solvent. A quantitative treatment is required for the solvation free energy since its difference between the reactant and product sides describes the solvent effect on the equilibrium constant in solution.

In order to explore a wide range of thermodynamic conditions, we calculate the

solvation free energy using the method of energy representation developed in previous works [5-7]. In the method of energy representation, the solvation free energy is provided exactly to second order in solvent density and its accuracy as an approximation is well established for both supercritical and ambient aqueous solutions. Since the approximate method needs the simulations only at the initial and final states of the process of solute insertion, its computational cost is much smaller compared to that in the (formally exact) free energy perturbation or thermodynamic integration method. Thus, the method of energy representation is suitable for studying the solvation effect over an extensive set of thermodynamic states including supercritical. In the present work, the solvation free energies of the reactive species appearing in Eqs. (1)-(3) are computationally obtained at hydrothermal conditions. The solvent effect on the equilibrium constants is then determined, and the dependence on the (solvent) density and temperature is discussed in connection to the interaction with the solvent water.

2. Procedures

To approach the equilibrium constant, the explicit treatment is necessary only for the reactant and product species. We let $\Delta\mu_i$ denote the solvent effect in the chemical potential of the i^{th} reactive species. We assume that the electronic structure and molecular geometry of the reactive species (solute) are not coupled with the solvent degrees of freedom. In this approximation, $\Delta\mu$ is the solvation free energy evaluated under the (effective) solute-solvent interaction and is expressed as

$$\exp\left(-\beta\Delta\mu\right)=\frac{\int d\mathbf{X}\exp\left(-\beta\left(V\left(\mathbf{X}\right)+U\left(\mathbf{X}\right)\right)\right)}{\int d\mathbf{X}\exp\left(-\beta U\left(\mathbf{X}\right)\right)} \tag{4}$$

where $\mathbf{X}$ represents the solvent configuration collectively, the solute-solvent and solvent-solvent interaction energies are $V(\mathbf{X})$ and $U(\mathbf{X})$, respectively, and β is the inverse of k_BT with the Boltzmann constant k_B and the temperature T. The solvent effect on the reaction equilibrium of interest is then described by the free energy change ΔW introduced as

$$\Delta W = \sum_{i:\text{product}} \nu_i \Delta\mu_i - \sum_{i:\text{reactant}} \nu_i \Delta\mu_i \tag{5}$$

with the stoichiometric coefficient ν_i. Correspondingly, the equilibrium constant K in the molarity unit is given by

$$K = K_0 \exp\left(-\beta\Delta W\right) \tag{6}$$

where K_0 is the equilibrium constant in the absence of solvent. In the present work, we construct K_0 from the standard free energies of formation of the relevant reactive species with an appropriate conversion of the concentration units into molarity.

The solvent is water. The water molecule was treated as rigid and nonpolarizable, and the SPC/E model was adopted as the intermolecular potential function between water molecules [8]. The thermodynamic states of interest are specified by the water density and temperature. Below the critical temperature, two groups of thermodynamic states were examined. In one of the groups, the temperature is varied at a fixed density of 1.0 g/cm^3, and in the other, the system is on the liquid branch of the (experimental) saturation curve of H_2O [9]. Above the critical temperature, the thermodynamic state was explored at a fixed temperature of 400 °C.

The solutes are formic acid (HCOOH), water (H_2O), hydrogen (H_2), carbon monoxide (CO), and carbon dioxide (CO_2). They appear as the reactive species in Eqs. (1)-(3). The intermolecular interaction was assumed to be pairwise additive and was described with Coulombic and Lennard-Jones terms. When the solute is HCOOH, the *cis* geometry in the notation of Ref. [10] was adopted (in which, the carbonyl O and the hydroxy H are on the same side) and the revised potential parameter set in Ref. [11] was employed. The parameters for H_2 were taken from Ref. [12]. CO and CO_2 were described as two- and three-site molecules, respectively, and the interaction sites were placed at the C and O positions. The C-O bond length was fixed at the gas-phase experimental value of 1.128 Å for CO and 1.160 Å for CO_2 [13]. The Lennard-Jones ε and σ for the C and O sites were set at the EPM values of Table I of Ref. [14], and the charge on the oxygen site was 0.02 for CO and -0.32 for CO_2 in the unit of elementary charge. These charges were determined to reproduce the experimental dipole and quadrupole moments, respectively, and the charge neutrality led to the value of the C-site charge. The Lennard-Jones part of the solute-water potential function was then constructed by the standard Lorentz-Berthelot combining rule [15].

For each solute and at each thermodynamic state, Monte Carlo simulations of the solution and pure solvent systems were conducted in the canonical ensemble. In the simulation of the solution system, the standard Metropolis sampling scheme was implemented by locating one solute molecule of interest and 500 water molecules in a cubic unit cell.

The simulation length was 500 K passes, where one pass corresponds to the generation of 500 configurations, and the method of preferential sampling was not adopted. The periodic boundary condition was employed in the minimum image convention, and the electrostatic potential was handled by the Ewald method with the surrounding medium of infinite dielectric constant. The screening parameter was then set to $5/L$, where L is the length of the unit cell, and 514 reciprocal lattice vectors were used. The truncation at $L/2$ was applied on the site-site basis to the real-space part of the electrostatic interaction in the Ewald method and the Lennard-Jones part of the intermolecular interaction. To simulate the pure solvent system, 500 water molecules were located in a cubic unit cell and were sampled for 100 K passes with the Metropolis scheme. The size of the unit cell was identical to that of the corresponding simulation of the solution system consisting of one solute molecule and 500 water molecules, and the boundary condition and Ewald sum parameters were the same as those for the solution system. The solvation free energy was then approximately evaluated in the method of energy representation according to the procedure presented in previous papers [6,7].

3. Results and Discussion

3.1. Solvation Free Energy In this section, we first observe the density and temperature dependence of the solvation free energy $\Delta\mu$. The dimensionless description will be provided because the solvation free energy appears in the form of $\beta\Delta\mu$ in the expression for the equilibrium constant given by Eqs. (5) and (6).

The density dependence of $\beta\Delta\mu$ at a fixed supercritical temperature of 400 °C is illustrated in Fig. 1 for typical cases of HCOOH, H_2O, CO, and CO_2. It is seen that the density dependence at constant temperature is qualitatively different between polar and nonpolar species [16]. When the solute is nonpolar, $\beta\Delta\mu$ increases steeply with the density in the range examined. In contrast, $\beta\Delta\mu$ of a polar solute is not a monotonic function of the density. It decreases in the low-density region and involves a minimum in the medium-density region. The density corresponding to the minimum is larger when the solute-water interaction is more favorable. In the high-density region, $\beta\Delta\mu$ of a polar solute increases with the density, and the density dependence of $\beta\Delta\mu$ is qualitatively common to the polar and nonpolar solutes.

The temperature dependence of $\beta\Delta\mu$ below the critical is illustrated in Fig. 2 for typical cases of H_2O, H_2, CO, and CO_2. $\beta\Delta\mu$ of each solute examined becomes less favorable (more positive) with the temperature elevation at a fixed density of 1.0 g/cm^3. The temperature dependence at constant density is weak for CO and H_2 and is strong for the polar solutes. To interpret this point, it is to be noted that $\beta\Delta\mu$ involves two competitive contributions from the repulsive and attractive interactions between the solute and solvent. The repulsive interaction is typically described as the excluded volume effect, and its strength in the dimensionless description is rather insensitive to the temperature variation. The attractive interaction for the solute molecules treated in this work, on the other hand, competes against the thermal energy and responds more sensitively to the temperature change. When the solute is nonpolar, the repulsive interaction makes the major contribution to $\beta\Delta\mu$ and leads to the weak temperature dependence at constant density. The attractive interaction is more effectively operative for a polar solute and is responsible for the stronger dependence of $\beta\Delta\mu$ on the temperature. It is of particular interest to see that $\beta\Delta\mu$ of CO_2 increases rapidly in the temperature elevation from 25 to ~150 °C and exhibits a weaker dependence at higher temperatures. As illustrated by using radial distribution functions in Ref. [17], the partial

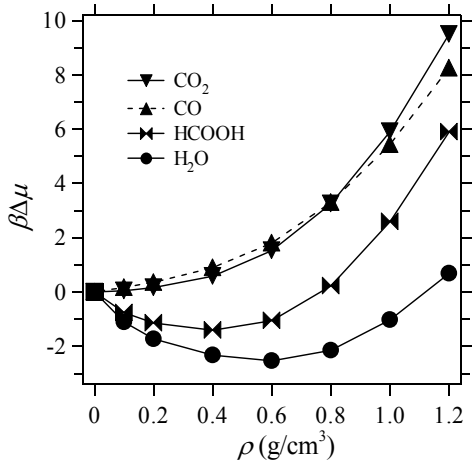

Fig. 1. $\beta\Delta\mu$ for HCOOH, H_2, CO, and CO_2 as a function of the solvent density ρ at a fixed temperature of 400 °C. The lines connecting the data are drawn for the eye guide. $\Delta\mu = 0$ holds at $\rho = 0$ by definition.

charges of CO_2 are large and the attractive interaction between CO_2 and water is stronger than that for typical nonpolar solutes such as CO and H_2. In the low-temperature region, the relatively sensitive dependence of $\beta\Delta\mu$ on the temperature is ascribed to the presence of the CO_2-water attraction. In the high-temperature region, in contrast, the repulsive interaction is more effective and the temperature dependence of $\beta\Delta\mu$ becomes close to that for other nonpolar solutes.

When the temperature dependence of $\beta\Delta\mu$ is examined for the nonpolar solutes on the saturation curve, the results in Fig. 2(b) are in agreement with the experimental observations [18]. The agreement includes, in particular, the inversions of $\beta\Delta\mu$ and the corresponding Henry's constant for CO and CO_2 at 100-200 °C. This illustrates the reliability of the present methodology. Above ~200 °C, the temperature elevation along the saturation curve leads to a less favorable $\beta\Delta\mu$ for a polar solute and to a more favorable $\beta\Delta\mu$ for a nonpolar solute. The opposite temperature dependence between the polar and nonpolar solutes is in contrast to the subcritical and high-density results in Figs. 1 and 2(a) that the temperature effect at constant density and the density effect at constant temperature are qualitatively similar between the polar and nonpolar solutes. When the temperature dependence along the saturation curve is viewed as a combination of the temperature effect at constant density and the density effect at constant temperature, the quantitative difference in the strengths of the two effects is responsible for the qualitative difference in the temperature dependence of $\beta\Delta\mu$ along the saturation curve. The temperature effect overwhelms the density effect when the solute is polar, while the contrary is operative for a nonpolar solute.

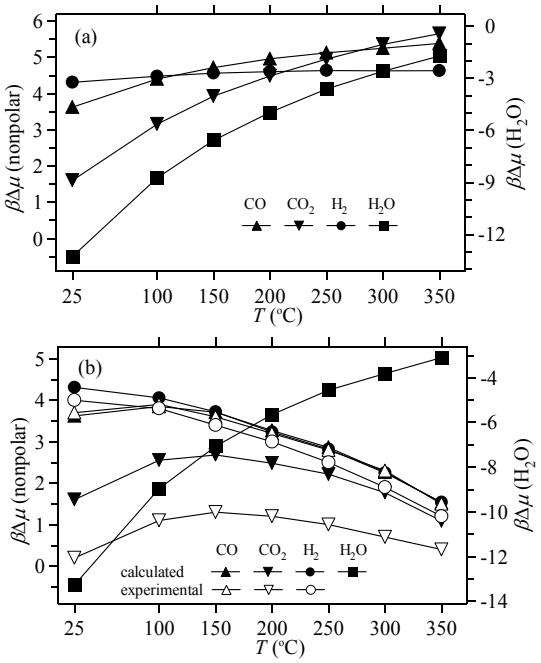

Fig. 2. $\beta\Delta\mu$ for CO, and CO_2, H_2, and H_2O as a function of the temperature T below the critical (a) at a fixed density of 1.0 g/cm^3 and (b) along the liquid branch of the saturation curve. In (b), the experimental data taken from Ref. [18] are also shown for comparison. The lines connecting the data are drawn for the eye guide.

3.2. Solvent Effect on the Reaction Equilibria In this subsection, we describe the solvent effect on the reaction equilibria of Eqs. (1)-(3). The description is provided in terms of a free energy change ΔW introduced by Eq. (5). We present the dependence of $\beta\Delta W$ on the (solvent) density and temperature. The dimensionless presentation is adopted since the equilibrium constant given by Eq. (6) involves the solvent effect in the form of $\beta\Delta W$.

In Fig. 3, we show $\beta\Delta W$ for the decomposition processes of formic acid expressed as Eqs. (1) and (2). The decarboxylation given by Eq. (2) corresponds to the conversion of one polar species into two nonpolar. The solvent water serves to suppress the production of nonpolar species, and its effect is stronger at a high density and/or a lower temperature. The decarbonylation is, on the other hand, a decomposition of one polar species into one polar and one nonpolar, as shown by Eq. (1). The dependence of $\beta\Delta W$ on the thermodynamic state is then relatively weak due to the cancellation of the $\beta\Delta\mu$ changes in the reactant and product sides. Actually, $\beta\Delta W$ for the decarbonylation reflects the delicate balance between the reactant and product $\beta\Delta\mu$, and is not necessarily monotonic in Fig. 3. When the reaction equilibrium is concerned in the absence of solvent, the corresponding standard free energy change is estimated to be ~-5 for Eq. (1) and ~-10 for Eq. (2) in the unit of the thermal energy k_BT [19]. These values are comparable to $\beta\Delta W$ in Fig. 3. The figure thus provides a possibility that the reaction equilibria for the HCOOH decompositions can be controlled by tuning the (solvent) density and temperature.

In the two decomposition pathways of HCOOH, the conversion between their product sides is called

the water-gas-shift reaction and is important both in fundamental physical chemistry and in fuel technology [4]. The water-gas-shift reaction given by Eq. (3) involves HCOOH as an intermediate [3], and its equilibrium constant determines the relative weights of the equilibrium decompositions of HCOOH into CO and CO_2. In Fig. 3, we also show $\beta\Delta W$ for the water-gas-shift reaction. The solvent favors the reactant side of Eq. (3) over the whole thermodynamic range examined, and acts more strongly at a higher density and/or a lower temperature. ΔW can actually be controlled on the order of 10 kcal/mol through the change in the (solvent) density and temperature. When no solvent is employed, the standard free energy change of Eq. (3) is estimated to be ~-5 kcal/mol, in favor of the CO_2 side [19]. This value is comparable in magnitude to ΔW in Fig. 3, and the favorable side of Eq. (3) can even be overturned by the solvent water. The strong solvent effect in the water-gas-shift reaction may be understood by noting that the reaction is a transformation of one polar and one nonpolar species into two nonpolar. When the density is increased at a fixed temperature of 400 °C, Fig. 3 shows that the equilibrium shifts to the reactant side, which involves the solvent species as a reactant. This is illustrates the significance of the solvation effect at high-temperature conditions.

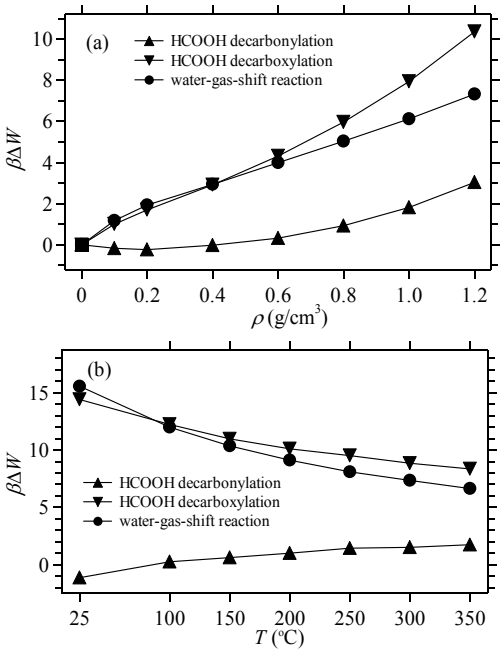

Fig. 3. $\beta\Delta W$ for HCOOH decarbonylation, HCOOH decarboxylation, and water-gas-shift reaction (a) as a function of the density ρ at a fixed temperature of 400 °C and (b) as a function of the temperature T below the critical at a fixed density of 1.0 g/cm^3. The lines connecting the data are drawn for the eye guide.

3.3. Equilibrium Constant In this subsection, we present the equilibrium constants for the C1 reactions expressed as Eqs. (1)-(3). In the absence of solvent, the equilibrium constant K_0 is constructed from the standard free energy of formation for each species of interest in the dilute gas condition [19]. K_0 is a function only of the temperature, and is combined through Eq. (6) with ΔW treated in the previous subsection to provide the equilibrium constant K in the presence of solvent. In the following, we adopt the molarity unit for K and K_0 and express them numerically in (a power of) mol/L. We will show ln$K$ and lnK_0 as functions of the temperature between 25 and 400 °C. The solvent density is then 1.0 and 0.4 g/cm^3 at 25 and 400 °C, respectively, and is set to the one on the liquid branch of the (experimental) saturation curve of H_2O at the other temperatures. The density dependence of ln$K$ will not be shown explicitly since it is solely carried by $\beta\Delta W$ and is parallel to the density dependence of -$\beta\Delta W$ with an

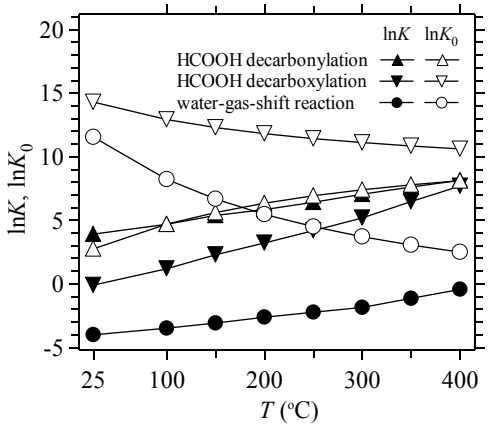

Fig. 4. The equilibrium constants ln$K$ and lnK_0 as functions of the temperature T for HCOOH decarbonylation, HCOOH decarboxylation, and water-gas-shift reaction. The solvent density is 1.0 and 0.4 g/cm^3 at 25 and 400 °C, respectively, and is set to the one on the liquid branch of the (experimental) saturation curve of H_2O at the other temperatures. The lines connecting the data are drawn for the eye guide.

offset of $\ln K_0$.

In Fig. 4, we show $\ln K$ and $\ln K_0$ for the decomposition processes of HCOOH described by Eqs. (1) and (2). The solvent is in favor of the reactant side of the decarboxylation given by Eq. (2). The solvent effect shown in Fig. 4 amounts to 5-10 in the $\ln K$ unit, and the temperature dependence of $\ln K$ is reversed from that of $\ln K_0$. The difference between $\ln K$ and $\ln K_0$ is relatively small, on the other hand, for the decarbonylation expressed as Eq. (1). Actually, the solvent can change the preference order of the decarbonylation and decarboxylation at equilibrium. In Fig. 4, $\ln K$ is larger for the decarbonylation than for the decarboxylation, while the opposite holds for $\ln K_0$. When the temperature is below ~300 °C, the $\ln K$ values for the HCOOH decompositions are less than ~5 in Fig. 4. The detection of HCOOH is then expected to be feasible in its hydrothermal decomposition mixture. Indeed, we were experimentally successful in detecting HCOOH and demonstrating its role as an intermediate of the water-gas-shift reaction [3].

In Fig. 4, we also show $\ln K$ and $\ln K_0$ for the water-gas-shift reaction. The solvent effect amounts to 5-15 at the thermodynamic states shown. Actually, the solvent can overturn the favorable side of the equilibrium in our convention of K and K_0. It is seen in Figs. 3 and 4 that although the CO_2 side is more stable in the absence of solvent, the CO side becomes more favorable with the solvent, except in the low-density supercritical region below ~0.3 g/cm^3. When the density is low enough and/or the temperature is high enough, K approaches to K_0. Figures 3 and 4 thus show that the equilibrium of the water-gas-shift reaction can be tuned by the (solvent) density and temperature. A strong solvent effect on the water-gas-shift reaction is further evidenced by the temperature dependence of the equilibrium constant. In Fig. 4, the temperature elevation leads to an increase of $\ln K$ and a decrease of $\ln K_0$ for the water-gas-shift reaction. The solvent effect is large enough to reverse the dependence of the equilibrium constant on the temperature. Actually, this temperature dependence of $\ln K$ is in agreement with the experimental observation at hydrothermal conditions that the CO_2 side is more favorable at higher temperatures [3]. The explicit treatment of the solvation effect is thus necessary to assess the temperature effect on the equilibrium of the water-gas-shift reaction.

Acknowledgements

This work is supported by the Grant-in-Aid for Scientific Research (No. 15205004) from Japan Society for the Promotion of Science and by the Grant-in-Aid for Scientific Research on Priority Areas (No. 15076205), the Grant-in-Aid for Creative Scientific Research (No. 13NP0201), and the NAREGI (National Research Grid Initiative) Project from the Ministry of Education, Culture, Sports, Science, and Technology. The work also benefits through the discussions with Dr. C. Wakai, Mr. Y. Nagai, Mr. K. Yoshida, and Ms. S. Morooka of Kyoto University.

References and Notes

[1] R. W. Shaw, T. B. Brill, A. A. Clifford, C. A. Eckert, and E. U. Franck, *Chem. Eng. News*, **69**, Dec. 23 issue 26 (1991).

[2] Since the backward reaction of Eq. (2) is called "hydration", we avoid the phrase "hydration" to denote the effect of intermolecular interaction between the solute and the solvent water. Instead, we use the phrase "solvation" to refer to the intermolecular interaction effects.

[3] K. Yoshida, C. Wakai, N. Matubayasi, and M. Nakahara, *J. Phys. Chem. A,* **108**, 7479 (2004).

[4] *Kirk-Othmer Encyclopedia of Chemical Technology, 4th ed.*, eds J. I. Kroschwitz and M. Howe-Grant (John Wiley & Sons, New York, 1991-1998).

[5] N. Matubayasi and M. Nakahara, *J. Chem. Phys.,* **113**, 6070 (2000).

[6] N. Matubayasi and M. Nakahara, *J. Chem. Phys.,* **117**, 3605 (2002); **118**, 2446 (2003) (erratum).

[7] N. Matubayasi and M. Nakahara, *J. Chem. Phys.,* **119**, 9686 (2003).

[8] H. J. C. Berendsen, J. R. Grigera, and T. P. Straatsma, *J. Phys. Chem.,* **91**, 6269 (1987).

[9] The International Association for the Properties of Water and Steam, *IAPWS Formulation 1995* (Fredericia, Denmark, 1996).

[10] P. Jedlovszky and L. Turi, *J. Phys. Chem. B,* **101**, 5429 (1997).

[11] P. Mináry, P. Jedlovszky, M. Mezei, and L. Turi, *J. Phys. Chem. B,* **104**, 8287 (2000).

[12] T. A. Bruce, *Phys. Rev. B*, **5**, 4170 (1972).

[13] *Kagaku Binran* (*Dictionary of Chemistry*)*, 5th and revised ed.*, eds Chemical Society of Japan (Maruzen, Tokyo, 2004, in Japanese).

[14] J. G. Harris and K. H. Yung, *J. Phys. Chem.,* **99**, 12021 (1999).

[15] J. P. Hansen and I. R. McDonald, *Theory of Simple Liquids, 2nd ed.* (Academic Press, London, 1986).

[16] Since the dipole moment is small, CO is categorized as nonpolar.

[17] H. Sato, N. Matubayasi, M. Nakahara, and F. Hirata, *Chem. Phys. Lett.,* **323**, 257 (2000).

[18] R. Fernández-Prini, J. L. Alvarez, and A. H. Harvey, *J. Phys. Chem. Ref. Data,* **32**, 903 (2003).

[19] NASA Glenn thermodynamic database, URL: http://cea.grc.nasa.gov.